Effects of preparation condition and particle size distribution on fumed silica gel valve-regulated lead–acid batteries performance[☆]

M.Q. Chen[a], H.Y. Chen[a,*], D. Shu[a], A.J. Li[a], D.E. Finlow[b]

[a] Key Lab of Technology on Electrochemical Energy Storage and Power Generation
in Guangdong Universities, School of Chemistry and Environment, South China Normal University, Guangzhou,
Guangdong 510006, PR China[1]
[b] Shawnee State University, Portsmouth, OH 45662, USA

ABSTRACT

The effects of three types of fumed silica on the electrochemical properties of gelled electrolytes have been investigated by means of cyclic voltammetry (CV), electrochemical impedance spectroscopy (EIS), transmission electron microscope (TEM) and the Brunauer, Emmett and Teller (BET) technique. The CV and EIS results show that a moderate mechanical dispersion of fumed silica in the H_2SO_4 solution has important effects on the electrochemical properties of the gelled electrolyte. The optimal mechanical dispersion time is closely related to the operating temperature during preparation of gel, as well as the silica particle size and its distribution. A high stirring rate improves the electrode capacity and decreases the viscosity of the gelled electrolyte. With moderate mechanical dispersion, gelled electrolytes prepared from different fumed silica particles exhibit equal electrode capacities.

© 2008 Elsevier B.V. All rights reserved.

1. Introduction

There are two types of technology for immobilizing the electrolyte in valve-regulated lead–acid (VRLA) batteries: one contains sulfuric acid solution in an absorptive glass-mat (AGM) separator; the other is a gelled electrolyte, which is a type of thixotropic colloid in a "soft solid" state [1]. Gelled electrolyte is prepared by mixing a gelling agent with sulfuric acid solution. The recombination reaction of oxygen takes place by rapid diffusion of oxygen from the positive to the negative plate through a network of microcracks. The batteries can therefore operate in a predominantly sealed manner, without any requirement for routine maintenance. SONNENSCHEIN dryfit batteries were the first GEL-VRLA batteries, and have been manufactured on a large scale since the 1950s [2].

The gelled electrolyte is the key factor affecting the performance of GEL-VRLA batteries. Major improvements in GEL-VRLA technology have been achieved over the past decade [3]. Several gelling

agents can be used to form a three-dimensional gel matrix; one is colloidal silica, which is inexpensive, can form a colloid with a long gelling time, and is easily loaded into the case. However, as revealed in some Chinese patents, gelled electrolytes formed from colloidal silica have the disadvantages of low capacity, low stability, poor thixotropy, and poor reliability under cyclic or deep-discharge condition [4–7]. Therefore, fumed silica is the commonly used gelling agent [3,8,9].

Fumed silica was first invented by Degussa in the 1940s. It is an exceptionally pure form of silicon dioxide, made by reacting silicon tetrachloride in an oxy-hydrogen flame. The process generates particles in the size range from 7 to 50 nm, which tend to link together by a combination of fusion and hydrogen bonding to form chain-like aggregates with high surface area. It is widely used as filler for strength reinforcement [10,11].

Because of the widespread utility of fumed silica, studies of the structure, and properties of its surfaces have been carried out by researchers for many years [12]. Careful analysis by a variety of methods such as IR [13,14], chemical probes, and NMR, indicated that the surface reactivity of the silica depends substantially on the quantity and structural arrangement of its surface hydroxyl groups. This, in turn, depends on the preparation process and modification method used for the silica [15,16]. Both "isolated" and "hydrogen-bonded" silanols (Si–OH) can be formed on the fumed silica surface, of which the "isolated" silanols are able to form an additional hydrogen bond [15].
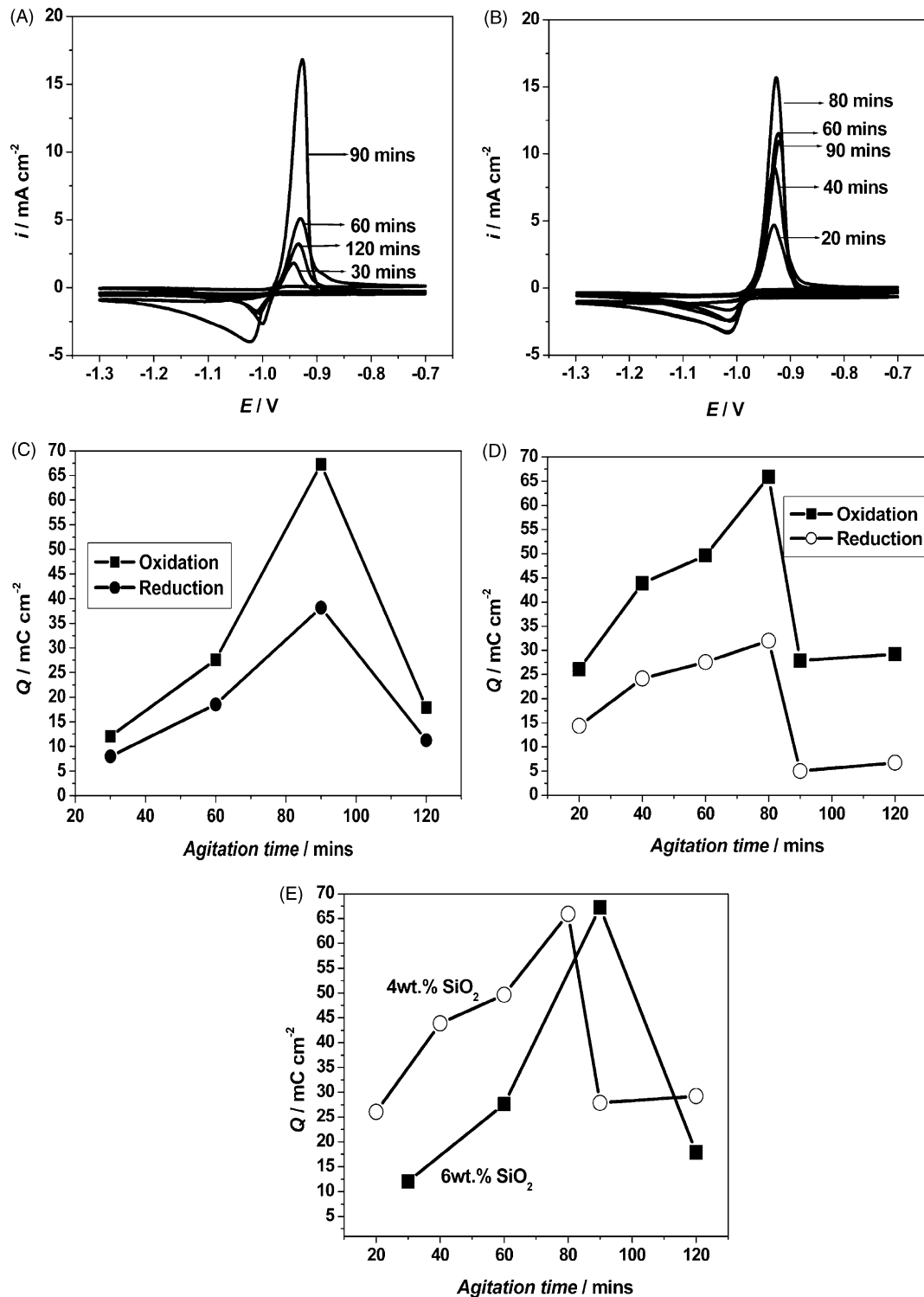
Fig. 1. CV curves of the lead electrode in gelled electrolytes (A200 silica, 3650 rpm, $30 \pm 1\,^{\circ}$C) prepared with different agitation times and silica contents: (A) 6 wt.% and (B) 4 wt.%. (C and D) Relationships between agitation time and redox capacity of the lead electrode derived from (A) and (B), respectively. (E) Oxidation capacities of the lead electrode in gels with different silica contents.

Fundamental studies on silica dispersions were initially based on aqueous media (see references in Raghavan et al. [17]). When the silica is dispersed in aqueous media, the isolated silanols may form hydrogen bonds with both the isolated silanols on other silica particles and water molecules, to give a silica gel or silica sol. As the isolated silanols form hydrogen bonds with

the water molecules, a "hydration force", a short-range, non-Deryaguin–Landau–Verwey–Overbeek (non-DLVO) repulsive force is generated. Strong hydration forces form a silica sol while weak hydration forces form a silica gel. Kamiya et al. [18] reported that the hydration force is a function of the diameter of the silica particles. Yoon and Vivek [19] demonstrated that the hydration force can
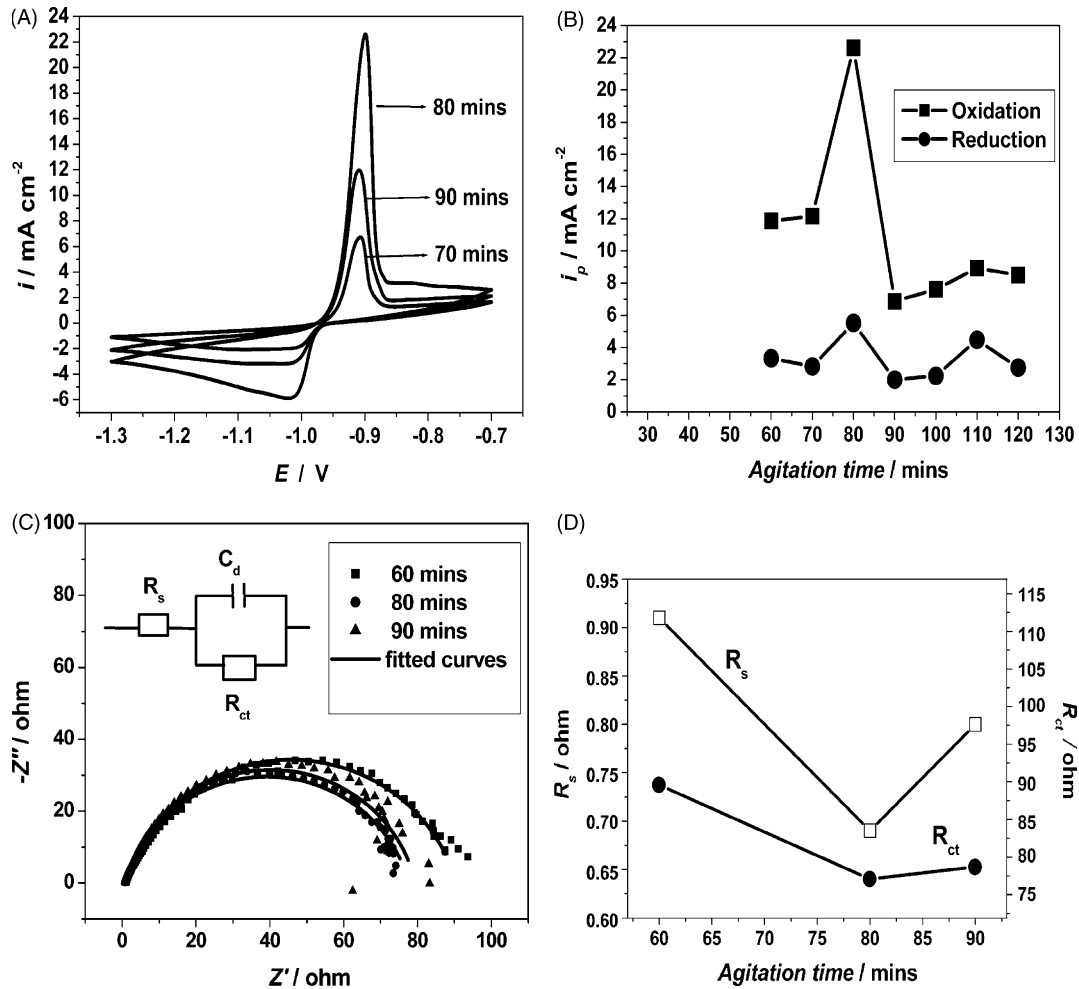
Fig. 2. CV and EIS results of the lead electrode in gelled electrolytes (6 wt.% A200, 4000 rpm, 25 ± 1 °C) prepared with different agitation times: (A) CV curves and (B) relationships between agitation time and redox peak current density of the lead electrode derived from (A). (C) Impedance spectra and (D) relationships between solution resistance (R_s) or charge-transfer resistance (R_{ct}) and agitation time derived from (C).

be eliminated in the presence of alcohols as a result of adsorption of the alcohols on the silica surfaces, displacing the water molecules, and disrupting the hydrogen-bonding network within the water layer around the silica particles.

When fumed silica is used in GEL-VRLA batteries, most of its isolated surface silanols link to form weak hydrogen bonds with each other. This gives a three-dimensional network gel structure, entrapping the sulfuric acid solution. The properties of this three-
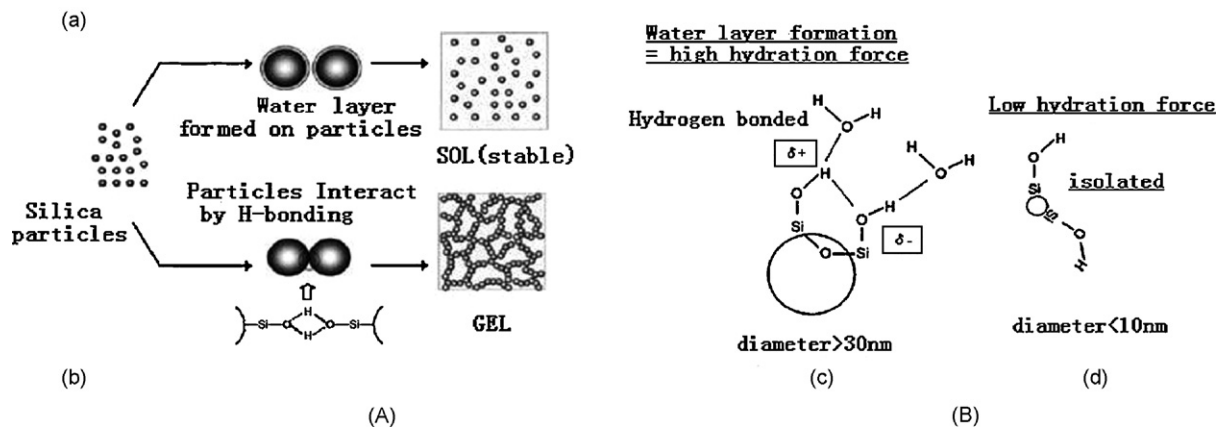

Fig. 3. Interaction effect between fumed silica particle: (A) effect of solvent: schematic representation of two possible scenarios that can occur in the case of silica particles dispersed in a aqueous liquid: (a) a strongly hydrogen-bonding liquid (water layer/hydration force is formed on the particles by hydrogen-bonding, resulting in a stable sol); (b) a weakly hydrogen-bonding liquid (the particles interact directly by hydrogen-bonding to form a gel) (reprinted by kind permission of Khan and co-workers [17]). (B) Effect of particle size: modeling of the effects of primary particle size on the surface silanol structure: the formation of a hydrated water layer and the hydration force (for particle diameters of (c) >30 nm and (d) <10 nm) (reprinted by kind permission of H. Kamiya and co-workers [18]).

Fig. 4. CV and EIS results of the lead electrode in gelled electrolytes (6 wt.% A200, 25 ± 1 °C) prepared with different agitation times and different stirring rates: at 3400 rpm: (A) CV curves, (B) impedance spectra, and (C) R_s and R_{ct} derived from (B); at 2400 rpm: (D) CV curves, (E) impedance spectra, and (F) R_s and R_{ct} derived from (E). (G) Relationships between agitation time and oxidation peak current density of the lead electrode in gelled electrolytes prepared with different stirring rates.
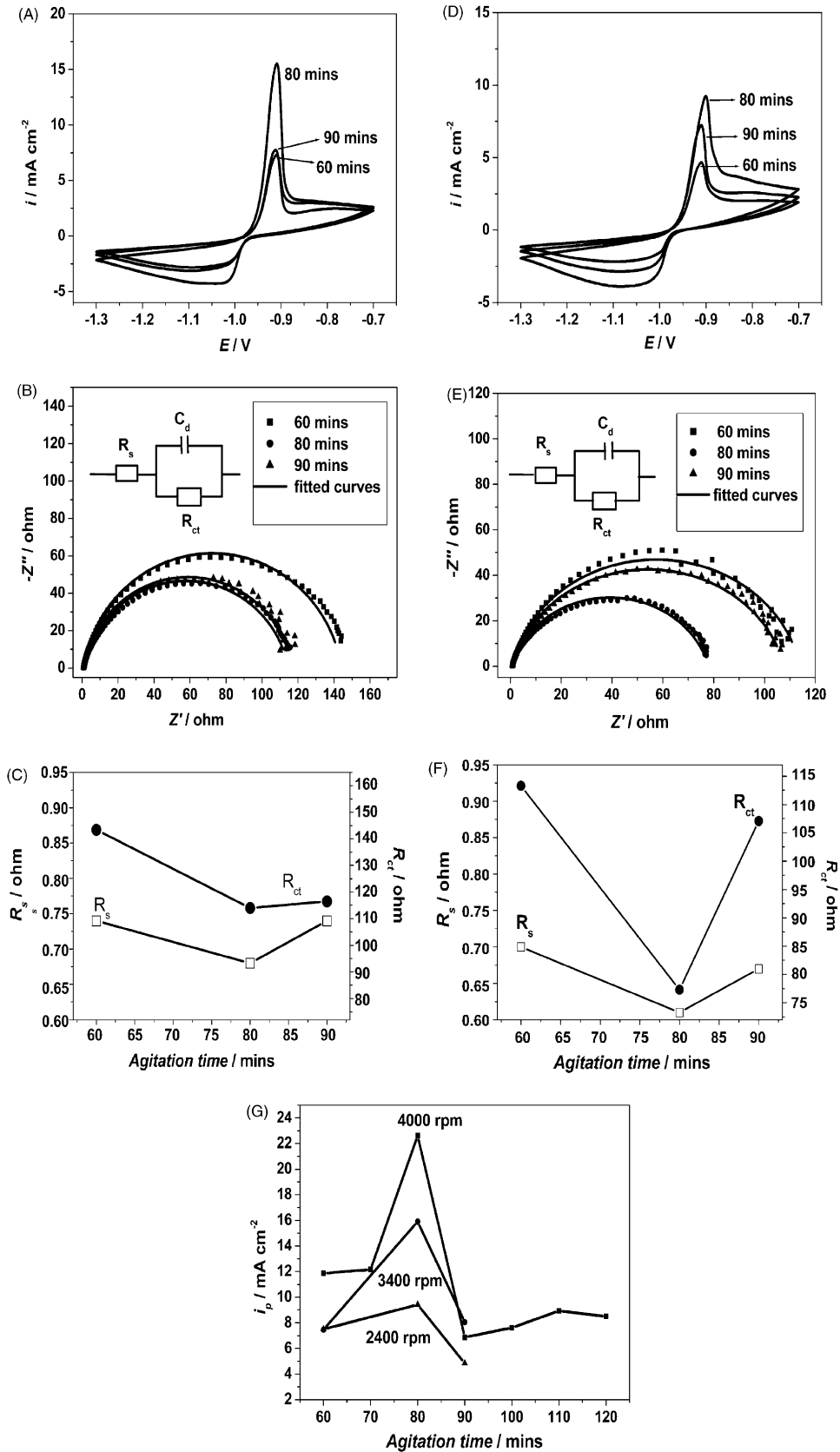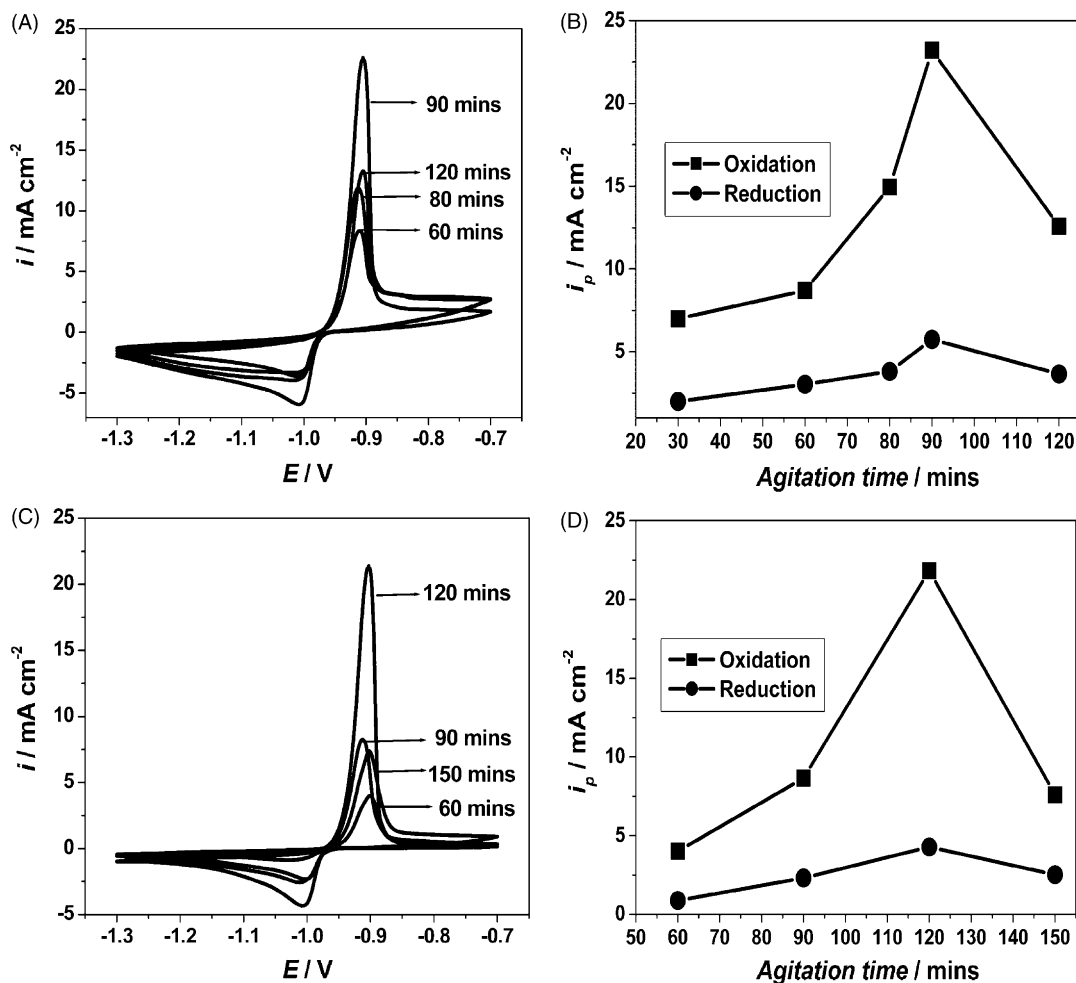
Fig. 5. CV results of the lead electrode in gelled electrolytes (6 wt.% A200, 4000 rpm) prepared with different agitation times and operating temperatures: 30 ± 1 °C: (A) CV curves and (B) relationships between agitation time and redox peak current density of the lead electrode derived from (A); 20 ± 1 °C: (C) CV curves and (D) relationships between agitation time and redox peak current density of the lead electrode derived from (C).

dimensional silica gelled electrolyte significantly affect the capacity and cycle life of GEL-VRLA batteries. Some researchers focused their effort on shortening gelling time, reducing the viscosity, and decreasing the internal resistance of the gelled electrolyte [20,21]. The optimal concentrations of: sulfuric acid solution, fumed silica, and various additives such as phosphoric acid have been investigated in an effort to improve the performance of the gels for VRLA batteries [22]. However, less concern has been placed on the dispersion properties of the fumed silica itself.

2. Experimental

A fundamental study was undertaken here to improve the performance of the gel, by taking advantage of the interfacial effects of fumed silica nanoparticles dispersed in H_2SO_4 solution. The intrinsic properties of fumed silica (concentration and particle size), plus the operating conditions used during the gelled electrolyte formation process (agitation time, stirring rate, and temperature) were investigated.

2.1. Physical characterization of fumed silica

The fumed silicas involved in this work were Aerosil 200, Aerosil 150 (produced by Degussa Co., Germany denoted as A200 and A150), and HL200 (produced by GBS Co., China) [23,24].

A JEM-2010HR transmission electron microscope (TEM) was employed to observe the morphology and microstructure of the silica particles. The BET specific surface area of the fumed silica particles was determined by a Micromeritics ASAP2020.

2.2. Preparation of the electrode and electrolyte

The working electrode was prepared by inserting a pure lead rod into a hard plastic tube and sealing with epoxy resin. A copper wire was welded to one end of the electrode. The opposite end was used as the flat, circular working surface, with a geometric area of 0.5 cm^2.

The gelled electrolyte was prepared by mixing fumed silica and 36 wt.% H_2SO_4 solution ($d = 1.285$ g mL^{-1}). The mixture was dispersed in a homogenizer at a high stirring rate to form a colloidal solution. Electrochemical testing was performed after gelation of the colloidal solution.

2.3. Electrochemical test

The cyclic voltammetry (CV) and electrochemical impedance spectroscopy (EIS) were carried out in a three-electrode configuration with an Hg/Hg$_2$SO$_4$, K$_2$SO$_4$ (saturated) reference electrode, and a platinum sheet as the counter electrode. The experiments were performed at room temperature using a PGSTAT30 (Autolab, Eco Echemie B.V. Company).

Prior to the experiment, the working electrode surface was polished with 1500# and 2000# waterproof silicon carbide papers. After washing with distilled water, the electrode was placed in the cell and cathodically polarized to remove the oxide film from its surface. CV curves were conducted over the potential range from -1.3 to -0.7 V at a scanning rate of $10\,\text{mV s}^{-1}$. The voltammogram of the 25th cycle was recorded in each experiment. EIS measurements were taken at the open-circuit potential (OCP) of -1.5 V in the frequency range 100 kHz–0.01 Hz, with an a.c. amplitude of 10 mV.

3. Results and discussion

3.1. Concentration of fumed silica

In GEL-VRLA batteries, fumed silica thickens and absorbs the electrolyte solution. The concentration of fumed silica is a key factor affecting the gelling properties. Kim et al. [25] concluded that the viscosity of a colloidal solution could be efficiently controlled by the fumed silica content. Lambert et al. [20] reported that the silica content of the electrolyte should be as low as possible in order to optimize the porosity of the colloidal particles, yet sufficiently high to develop and maintain a stable gel structure. It was suggested that with increasing silica content, the gelling time shortens and the structure of the gel becomes more compact. Consequently, the diffusion of reactants is inhibited, and the lead electrode capacity tends to diminish. In addition, the ohmic resistance and the charge-transfer resistance increase with higher silica content [21]. However, in this study it is demonstrated that the dispersion of fumed silica is also an important factor in determining the electrochemical performance of a gelled electrolyte. This had been overlooked in previous investigations.

Fig. 1 shows the CV curves for the lead electrode in gelled electrolytes containing 6 wt.% (Fig. 1A) and 4 wt.% (Fig. 1B) A200 fumed silica. The gels were prepared with different agitation times at a stirring rate of 3650 rpm, with an operating temperature of $30 \pm 1\,^\circ\text{C}$. The lead electrode capacity of gels prepared with the same silica content varies with agitation time. When the silica content is 6 wt.% (Fig. 1A and C), an agitation time of 90 min is required to reach the highest capacity, whereas for a silica content of 4 wt.% (Fig. 1B and D), only 80 min are required. With optimal dispersion, however, the oxidation capacities of gelled electrolytes prepared with 6 and 4 wt.% silica are equal (Fig. 1E).

Since the dispersion of the fumed silica plays such an important role in the electrochemical properties of the gelled electrolyte, a more detailed study of the effects of the factors used during the gel making progress (see Section 3.2) was undertaken.

3.2. Mechanical dispersion of fumed silica

3.2.1. Agitation time

In this section, CV and EIS were employed to evaluate the electrochemical performance of the gels. CV results for gelled electrolytes prepared at a stirring rate of 4000 rpm are shown in Fig. 2A and B. Initially, the redox peak currents (related to redox capacities) increase with increasing agitation time, reaching a maximum at about 80 min, before decreasing. It can be concluded that a lower or higher agitation time (within 10 min of the optimum) will lead to a sharp decrease in the peak current (capacity) of the lead electrode.

The impedance spectra (performed at -1.5 V) for gelled electrolyte prepared at a stirring rate of 4000 rpm is shown in Fig. 2C. The results can be fitted well by the equivalent circuit included. R_s represents the ohmic resistance, made up of the resistance of the corrosion products deposited on the electrode surface, the resistance of the electrolyte, and the resistance of the electrical
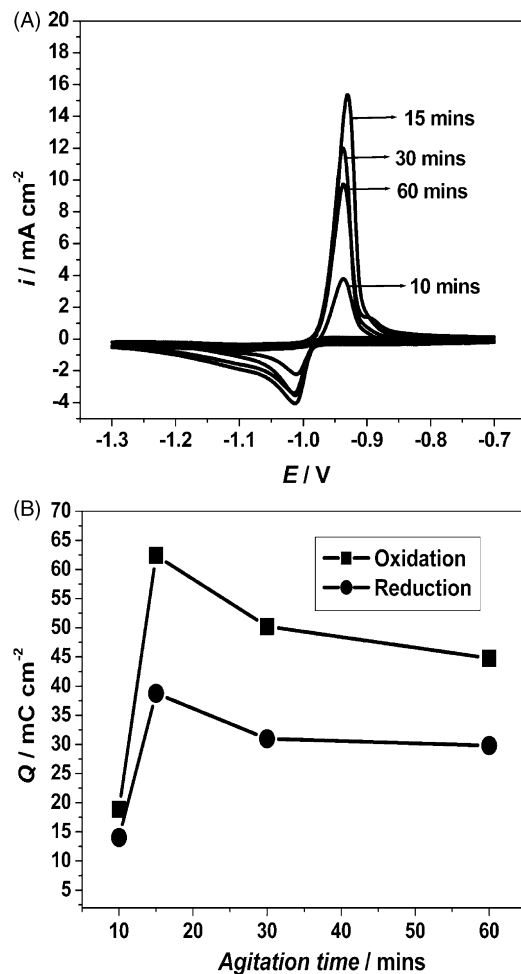

Fig. 6. CV results of the lead electrode in gelled electrolytes (6 wt.% HL200 silica, 3650 rpm, $30 \pm 1\,^\circ\text{C}$) prepared with different agitation times: (A) CV curves and (B) relationships between agitation time and redox capacity of the lead electrode derived from (A).

connections to the electrode. R_{ct} is the charge-transfer resistance of the rate-controlling electrochemical reaction of the corrosion process. C_d is the double-layer capacitance [26]. It can be seen that the solution resistance (R_s) and charge-transfer resistance (R_{ct}) of the gel reach a minimum with the optimal agitation time (80 min) (Fig. 2D). Therefore, the EIS results are consistent with the results obtained from the CV study.

The observed dispersion behavior of fumed silica is closely related to the nature of the dispersion medium [27]. As reported by Raghavan et al. [17], a silica gel or a sol will be formed according to the properties of the dispersion medium. Sulfuric acid solution is a weak, hydrogen-bonding, aqueous media because the SO_4^{2-} ion plays a steric hindrance role. When fumed silica is dispersed in it, a colloidal silica gel is formed (Fig. 3A). The silica particles are envisioned to directly interact with each other through hydrogen-bonding interactions between the surface silanol (Si–OH) groups. It is believed that hydrogen bonds, not Van der Waals interactions are responsible for the gel formation. Therefore, a uniform distribution of silica particles in sulfuric acid would help to optimize the interaction of surface silanol (Si–OH) groups on the silica particles, resulting in the formation of a uniform, microscopic, three-dimensional gel structure, which provides the gelled electrolyte with high capacity and low inner resistance.
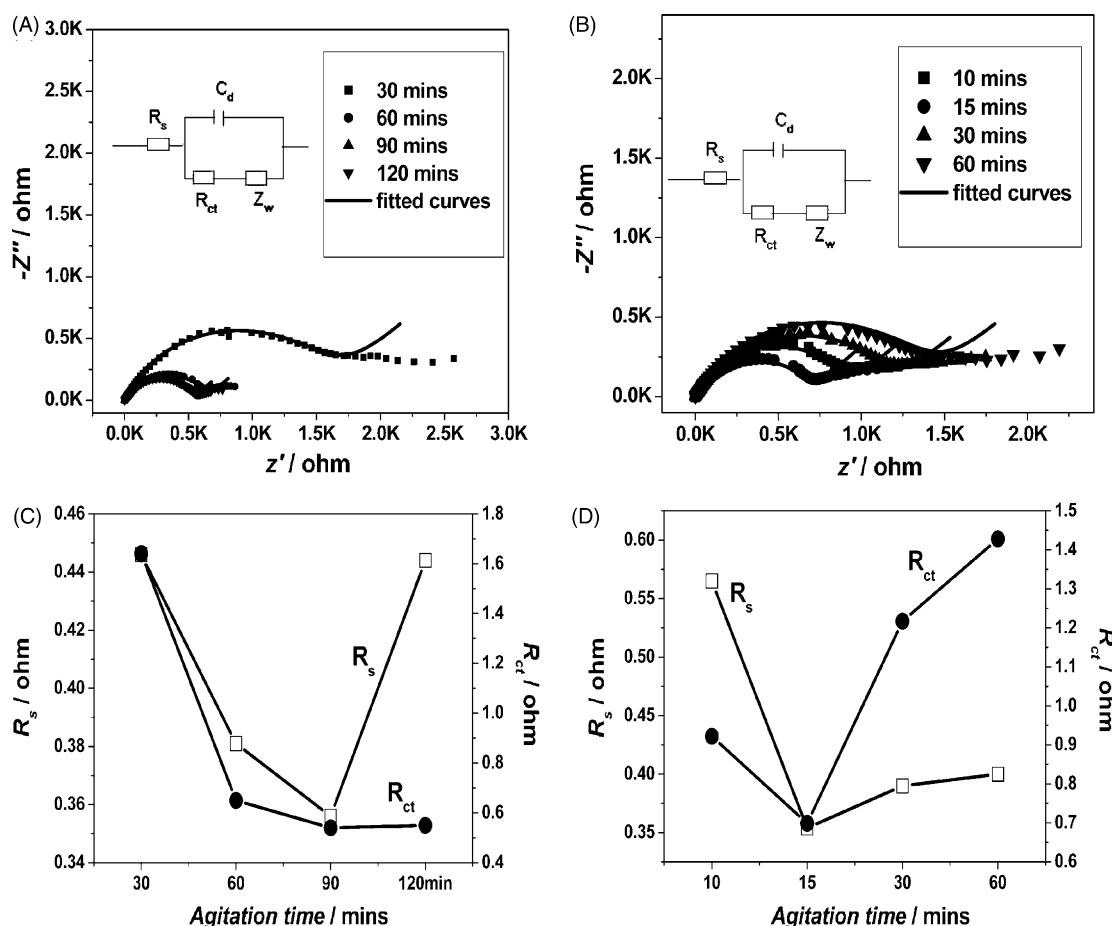
Fig. 7. Impedance spectra results of the lead electrode in gelled electrolytes (6 wt.% silica, 3650 rpm, $30 \pm 1\,°C$) prepared with different agitation times and different silicas: (A) A200; (B) HL200; (C and D) R_s and R_{ct} derived from (A) and (B), respectively.

Practically, the uniformity distribution of silica particles can be controlled by two processes: the dispersion of the fumed silica conglomeration and the gelling process. With increasing agitation time, the aggregation is separated gradually to form a moderate three-dimensional web structure; in parallel, however, the colloidal solution is gelling. Balancing these two competing processes necessitates an optimal agitation time for moderate gel structures.

3.2.2. Stirring rate

The CV and EIS results for gelled electrolytes prepared at stirring rates of 3400 and 2400 rpm are shown in Fig. 4. They confirm that gels prepared with the optimal dispersion time (80 min) possess the lowest internal resistance and highest redox peak current (capacity).

Fig. 4G also indicates that the optimal agitation time for fumed silica dispersed in H_2SO_4 solution is independent of the stirring rate. However, the redox peak currents were affected by the stirring rate. The higher stirring rates yielded larger electrode oxidation peak currents. When nanoparticles have a heterogeneous distribution, they become distributed homogeneously as the particles diffuse from high to low concentration areas. Increasing the stirring rate yields a higher diffusion rate, which appears to be beneficial to the microstructure of the gel.

3.2.3. Operating temperature

CV results for gelled electrolytes prepared at different temperatures are shown in Fig. 5. The optimal agitation time is about 90 min at 30 °C (Fig. 5A and B), whereas it is about 80 min at 25 °C (Fig. 2A and B). These phenomena can be explained by the previous research. Ponton et al. [28] stated that apparent activation energy could be determined from the temperature dependence of gelation time. Kim et al. [25] pointed out that temperature affected the viscosity of the fumed silica dispersions. In the field of GEL-VRLA batteries, the influence of temperature on the gelling process follows an Arrhenius relationship (*i.e.* the rate of gelation doubles with every 10 °C rise in temperature) [20]. Park et al. [29] revealed that the gel strength increases with temperature. Therefore, the optimal dispersion time is longer at 30 °C than at 25 °C.

However, at 20 °C (Fig. 5C and D) the optimal dispersion time is significantly longer, at 120 min. Thus, both the gelation and dispersion rates of the fumed silica conglomeration are affected by temperature. Higher temperature is beneficial for dispersion of the fumed silica conglomeration because of higher diffusion rates. The optimal agitation time is therefore mainly determined by the operating temperature. At a specific temperature, however, deviations from the optimum agitation time would lead to a reduced lead electrode capacity.

3.3. Fumed silica from different companies

It is well known that gelled electrolyte prepared from imported fumed silica has the advantages of high capacity, excellent recyclability, and long service life. But imported fumed silica is expensive, and it is difficult to fill the cell with the resulting high viscosity gel [30,31]. In this study, attempts were made to use domestically

produced fumed silica instead. It was found that there are great differences in the electrochemical properties of gelled electrolytes prepared with fumed silicas from different sources. Compared to imported fumed silica, gels prepared from domestic fumed silica have low battery capacity and weak thixotropic properties. A series of experiments was designed to investigate the reasons for the differences.

As found in this study (see Section 3.1), an optimal agitation time of 90 min is required for 6 wt.% A200 fumed silica (Fig. 1). However, at the same conditions, only about 15 min are required (Fig. 6) for HL200 fumed silica. Impedance spectra of gels made from A200 and HL200 silica, recorded at OCP, are provided in Fig. 7A and B. A semi-circular curve at high frequency and straight line at low frequency are observed in all cases. The radius of the high frequency semi-circle in the plot represents the charge-transfer resistance of the electrochemical process [32]. The low frequency straight line indicates a diffusion-controlled process. The intercept of the semi-circle with the real axis primarily indicates the ohmic resistance of the solution. The parameters derived according to the equivalent circuit are also provided (Fig. 7C and D). Gels prepared with the optimal agitation time possess the highest electrode capacity as well as minimal R_s and R_{ct} for both A200 and HL200 silica. The conclusions from the EIS results recorded at OCP are consistent with those recorded at −1.5 V (see Section 3.2.1).

Though they experienced different optimal agitation times, the lead electrode in these gelled electrolytes (prepared from HL200 or A200) demonstrated almost equal electrochemical capacities (Fig. 8). Legrand et al. [15] reported that the conglomeration behavior of fumed silica depends substantially on the structural arrangement of its surface. Burneau et al. [33–36] found that the amount and distribution of hydroxyl groups on fumed silica are closely related to the preparation methods. Therefore, there may be some differences in the hydroxyl group quantity or types for A200 and HL200 silica. Also, the behavior of fumed silica has a strong relationship with its particle size.

The average diameters of A200 silica particles observed from Fig. 9 are consistently around 12 nm, whereas the diameters of HL200 silica are more variable: from 10 to 20 nm. Thus, the average particle size of A200 silica is smaller than that of HL200, plus A200 fumed silica particles possess a more uniform particle diameter distribution. This result coincides with the BET specific surface area measurements (Table 1). The A200, with a smaller average particle size, possesses a higher specific surface area. As a result, A200 fumed silica agglomerates more readily and requires greater agitation time to form a uniform gel structure.

It is suggested that the two main factors responsible for the low gelling ability and low capacity of the gel prepared from HL200 are: a less than optimal mechanical dispersion of the fumed silica, leading to a weak thixotropic nature and low capacity of the gelled electrolyte; the uneven particle diameter distribution, leading to low gelling ability. The mechanisms of how the particle diameter and its distribution affect the dispersion and aggregation behavior of fumed silica will be discussed in detail in Section 3.4.

3.4. Particle size of fumed silica

Nanomaterials have many particle size-dependent properties. It was reported that silica nanoparticles could be adapted to specific

Table 1
BET specific surface area of different types of fumed silica particles

Type of fumed silica	BET specific surface area ($m^2\,g^{-1}$)
HL200	168.6
A200	213.9
A150	159.8

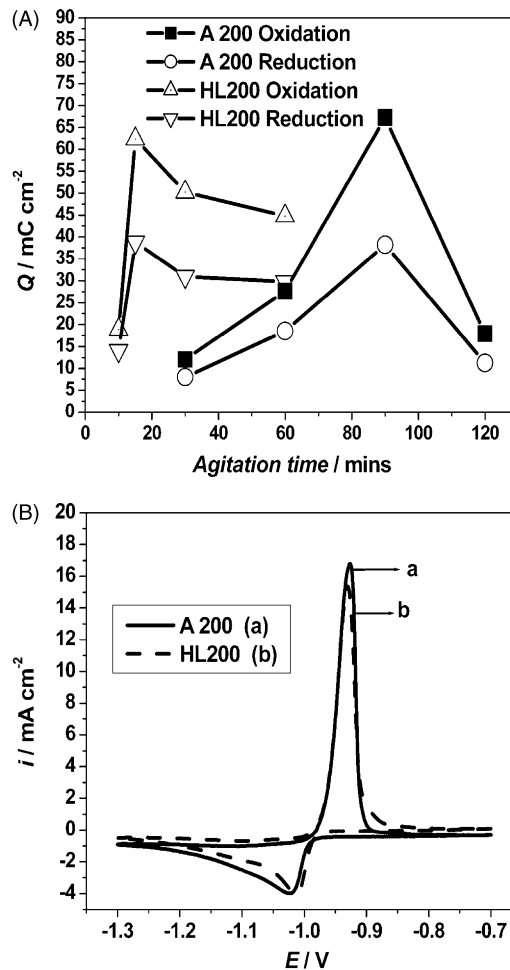**Fig. 8.** CV results of the lead electrode in gelled electrolytes (6 wt.% silica, 3650 rpm, 30 ± 1 °C) prepared from different silicas: (A) CV curves of: (a) A200 for 90 min and (b) HL200 for 15 min; (B) relationships between agitation times and redox capacity of the lead electrode.

applications in biotechnology by size control [37,38]. Researchers have already published information about the influence of silica diameter on gel properties. Mao et al. [7,39] pointed out that gels formed by silica with particle diameters <5 nm had short gelling times, strong gel strength, and poor thixotropy. However, with silica particle diameters >50 nm the gel strength was too weak to immobilize the electrolyte. Kamiya et al. [18] reported that hydration forces are responsible for this effect in water. The experiment designed in this section aims to determine how the particle size and size distribution of fumed silica affect its dispersion and aggregation behavior in sulfuric acid solution.

The A200 and A150 involved in this work have uniform particle size distributions with average diameters of about 10 and 20 nm, respectively. The dispersion behavior of 6 wt.% A200, 6 wt.% A150, and 6 wt.% fumed silica mixture (with 3 wt.% A200 and 3 wt.% A150) were studied using CV. The fumed silica was dispersed at 4000 rpm and 25 °C. It was found that for fumed silica with a particle diameter of 10 nm, an optimal agitation time of 80 min is required (Fig. 10). For fumed silica with 20 nm average diameter, agitation time does not have a significant effect on the lead electrode capacity. However, 40 min are required for fumed silica containing 50% 10 nm particles and 50% 20 nm particles. The optimal mechanical agitation time therefore has a close relationship with the particle size of fumed silica.
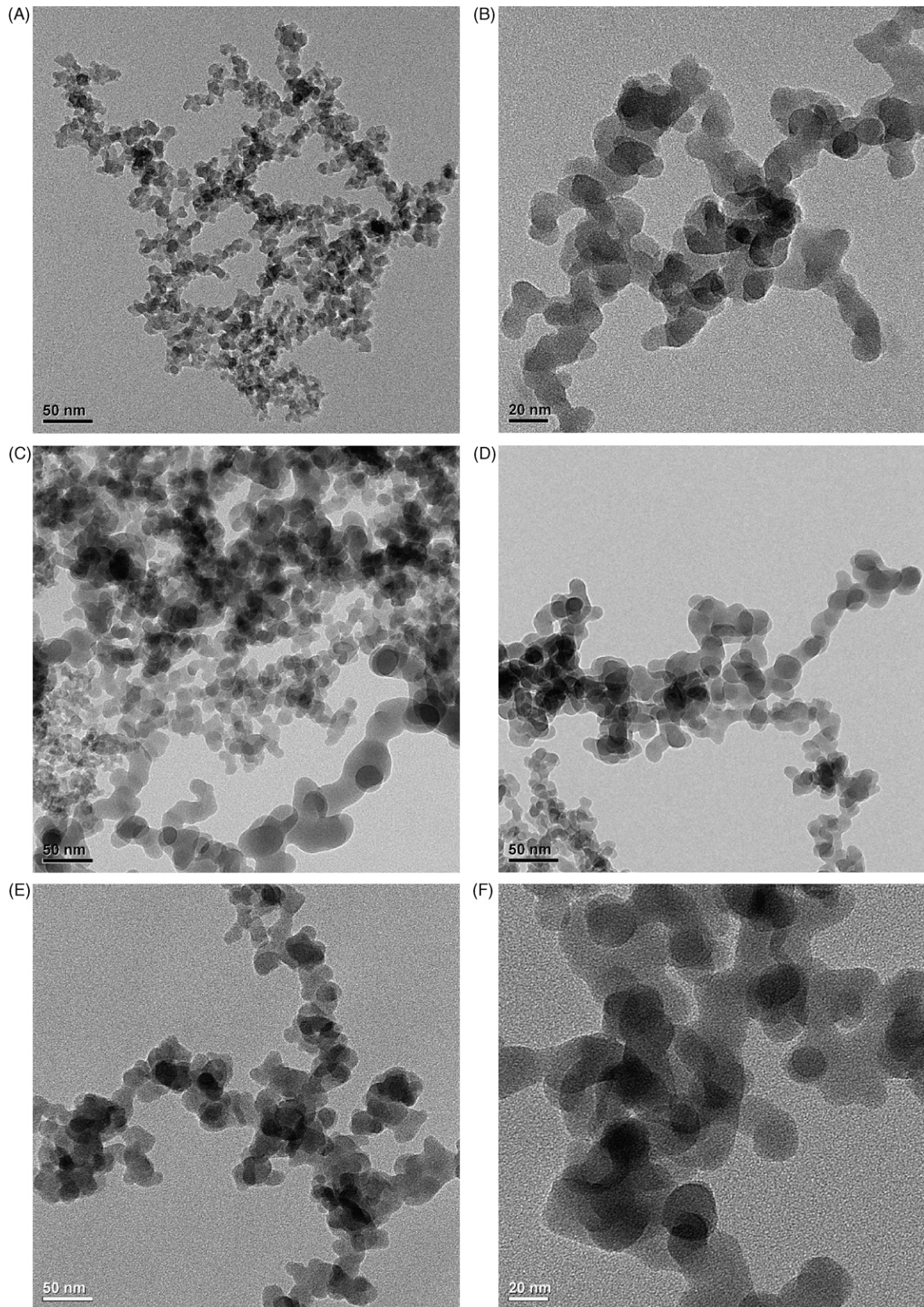
Fig. 9. TEM images of different fumed silicas: A200 particles: (A) 50,000× and (B) 100,000×; HL200 particles: (C and D) 50,000×; A150 particles: (E) 50,000× and (F) 100,000×.
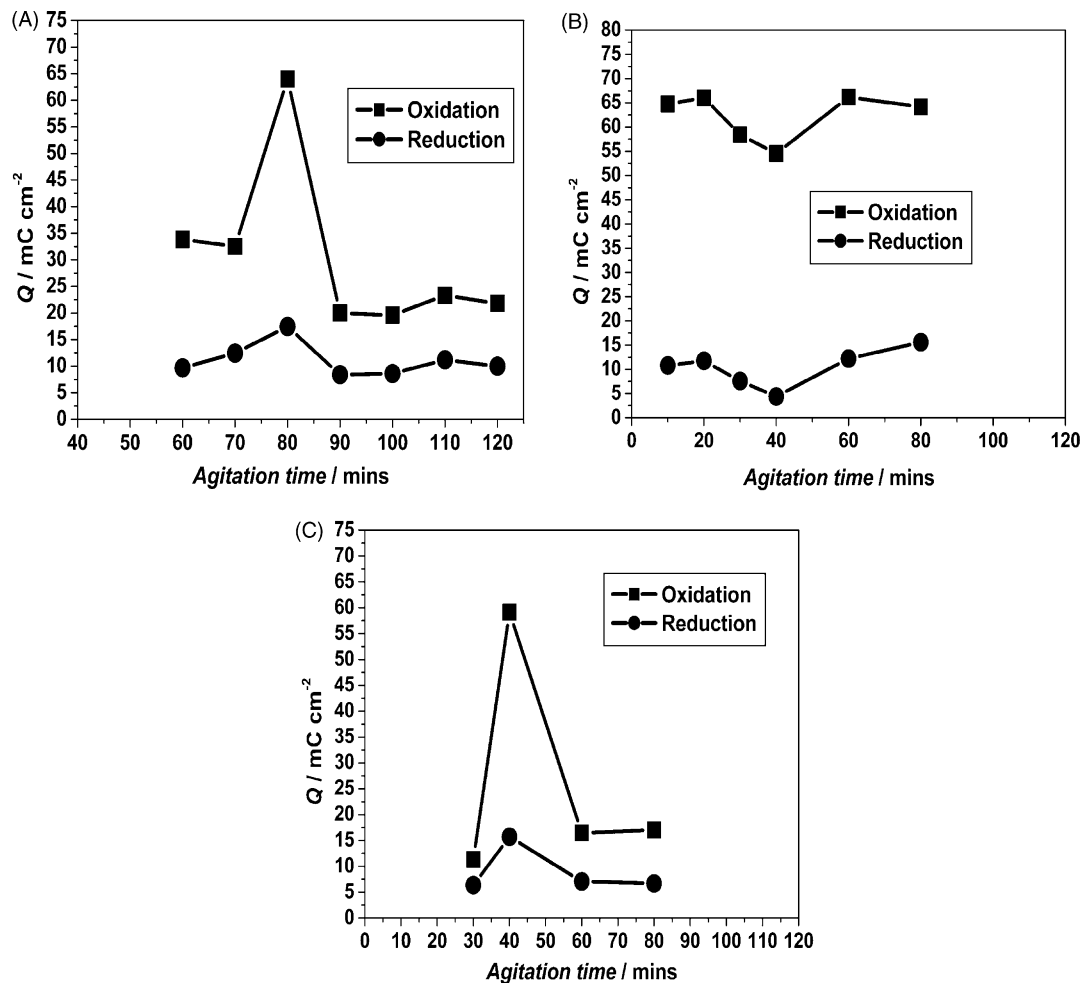
Fig. 10. Relationships between agitation time and redox capacity of the lead electrode in gelled electrolytes (4000 rpm, 25 ± 1 °C) prepared from different silicas: (A) 6 wt.% A200, (B) 6 wt.% A150, and (C) 3 wt.% A200 and 3 wt.% A150.

Kamiya et al. [18] suggest that fumed silicas with relative large particle size ($d \geq 20$ nm) have more hydrogen-bonded silanols and fewer isolated silanols on their surface. The hydrogen-bonded water layer on the particle surface causes the hydration force among these particles. This additional hydration force helps to prevent aggregation of the fumed silica particles (Fig. 3B). However, when the particle diameter decreases to 10 nm, the surface density of the isolated silanols increases, the hydration force among silica nanoparticles disappears and strong agglomerations are formed. As a result, a long optimal agitation time is required. The optimal agitation time decreases as the proportion of ~10 nm fumed silica particles decreases. With optimal mechanical dispersion, an almost equal redox capacity can be obtained with gelled electrolytes prepared from fumed silica with different particle sizes (Fig. 10).

As indicated in Section 3.2.1, it is believed that hydrogen-bonding between isolated silanols is responsible for gel formation. So, the strength of a gel prepared from relatively large fumed silica particles (≥ 20 nm) is poor because of few isolated silanols on the surface. Theoretically, gel strength is enhanced as the proportion of ~10 nm fumed silica particle increases.

4. Conclusions

Mechanical dispersion of fumed silica nanoparticles was investigated as an important factor in the preparation of high performance gelled electrolytes. Optimal mechanical agitation time is the key factor in preparing gelled electrolytes with high lead electrode redox peak current (capacity) and low internal resistance. Deviations of ±10 min from the optimal agitation time cause a 40–70% decrease in lead electrode capacity. For a particular type of fumed silica at a specific concentration, the optimal mechanical agitation time is determined by the operating temperature. High stirring rates increase the electrode capacity of the gelled electrolyte. For fumed silica from different producers, optimal agitation time varies because of different particle size distributions. Fumed silica with a diameter of ~10 nm tends to aggregate easily, while aggregation for diameters ≥ 20 nm is more difficult. The optimal agitation time is determined by the proportion of smaller silica particles ($d \leq 10$ nm). Equal lead electrode capacity can be obtained for gelled electrolytes prepared from fumed silica with different particle sizes by utilizing the optimal mechanical dispersion.

References

[1] H. Tuphorn, J. Power Sources 46 (1993) 361–373.
[2] D. Berndt, J. Power Sources 100 (2001) 29–46.
[3] V. Toniazzo, J. Power Sources 158 (2006) 1124–1132.

[4] L.C. Zhou, CN 1169040A (1997).
[5] Y.F. Zhang, H.Q. Wang, CN 1061113A (1992).
[6] M. Chen, CN 1163492A (1997).
[7] X.X. Mao, H. Zhang, G.C. Xu, CN 1503393A (2004).
[8] R. Wagner, in: D.A.J. Rand, P.T. Moseley, J. Garche, C.D. Parker (Eds.), Valve-regulated Lead–Acid Batteries, Elsevier, Amsterdam, 2004, p. 447.
[9] M.L. Soria, J.C. Hernández, J. Valenciano, A. Sánchez, F. Trinidad, J. Power Sources 144 (2005) 473–485.
[10] W.H. Ruan, X.B. Huang, X.H. Wang, M.Z. Rong, M.Q. Zhang, Macromol. Rapid Commun. 27 (2006) 581–585.
[11] W.H. Tan, K.M. Wang, X.X. He, X.J. Zhao, T. Drake, L. Wang, R.P. Bagwe, Med. Res. Rev. 24 (5) (2004) 621–637.
[12] C.C. Liu, G.E. Maciel, J. Am. Chem. Soc. 118 (1996) 5103–5119.
[13] B.A. Morrow, I.A. Cody, J. Phys. Chem. 80 (1976) 1998.
[14] I.D. Gay, A.J. McFarlan, B.A. Morrow, J. Phys. Chem. 95 (1991) 1360.
[15] A.P. Legrand, H. Hommel, A. Tuel, H. Balard, E. Papirer, P. Levitz, M. Czerni-chowski, R. Erre, H. Van Damme, J.P. Gallas, J.F. Hemidy, J.C. Lavalley, O. Barres, A. Burneau, Y. Grillet, Adv. Colloid Interf. Sci. 33 (1990) 91.
[16] G.D. Parfitt, K.S.W. Sing, Characterization of Powder Surfaces, Academic Press, New York, 1976, p. 403.
[17] S.R. Raghavan, H.J. Walls, S.A. Khan, Langmuir 16 (2000) 7920–7930.
[18] H. Kamiya, M. Mitsui, H. Takano, S. Miyazawa, J. Am. Ceram. Soc. 83 (2) (2000) 287–293.
[19] R.H. Yoon, S. Vivek, J. Colloid Interf. Sci. 204 (1998) 179–186.
[20] D.W.H. Lambert, P.H.J. Greenwood, M.C. Reed, J. Power Sources 107 (2002) 173–179.
[21] L. Wu, H.Y. Chen, X. Jiang, J. Power Sources 107 (2002) 162–166.
[22] L. Torcheux, P. Lailler, J. Power Sources 95 (2001) 248–254.
[23] O. Jache, H. Schroeder, US Patent 4,414,302 (1983).
[24] A.M. Chreitzberg, F.J. Chiacchio, US Patent 4,587,718 (1987).
[25] S. Kim, J. Jang, O. Kim, Polym. Test. 17 (1998) 225–235.
[26] M.P. Vinod, K. Vijayamohanan, J. Power Sources 89 (2000) 88–92.
[27] M. Kawaguchi, A. Mizutani, Y. Mastushita, T. Kato, Langmuir 12 (1996) 6179–6183.
[28] A. Ponton, S. Warlus, P. Griesmar, J. Colloid Interf. Sci. 249 (2002) 209–216.
[29] J. Park, S.B. Park, S.M. Yang, W.H. Hong, C.R. Choi, J.H. Kim, J. Non-Cryst. Solids 351 (2005) 2352–2357.
[30] H.Y. Chen, S.Y. Zhu, S.Y. Liang, Chin. LABAT Man 1 (2002) 5–8.
[31] Z.G. Guo, H.M. Li, Chin. J. Power Sources 130 (2) (2006) 130–132.
[32] A.J. Bard, L.R. Faulkner, Electrochemical Methods Fundamentals Application, John Wiley, New York, 1980, p. 131.
[33] M. Zaborski, A. Vidal, G. Ligner, H. Balard, E. Papirer, A. Burneau, Langmuir 5 (1989) 447–451.
[34] A. Burneau, O. Barres, J.P. Gallas, J.C. Lavalley, Langmuir 6 (1990) 1364–1372.
[35] A. Burneau, O. Barres, A. Vidal, H. Balard, G. Ligner, E. Papirer, Langmuir 6 (1990) 1379–1395.
[36] J.P. Gallas, J.C. Lavalley, A. Burneau, O. Barres, Langmuir 7 (1991) 1235–1240.
[37] S. Santra, K. Wang, R. Tapec, W. Tan, J. Biomed. Opt. 6 (2001) 160–166.
[38] M. Qhobosheane, S. Santra, P. Zhang, W. Tan, Analyst 126 (2001) 1274–1278.
[39] X.X. Mao, H. Zhang, G.C. Xu, Z. Tang, CN 2598159Y (2004).